LU-TP 22-03
January 2022

Computational modelling of photosynthetic excitons coupled to a microcavity

Ilmari Turunen

Department of Astronomy and Theoretical Physics, Lund University

Master thesis supervised by Tönu Pullerits

LUND UNIVERSITY

Abstract

Cavity quantum electrodynamics (QED) is a theory that is used for describing the interaction between matter and cavity modes. Not until relatively recently, cavity QED has been extended to the study of photosynthetic light-harvesting complexes (LHCs). Multiple phenomena unique to strongly cavity-coupled molecular systems have also been observed in LHCs in cavities. Of such phenomena, one is the formation of highly coherent states delocalized among thousands of molecules. These states have a partial light character, and are known as molecular polaritons. In this thesis, I explore the formation of polaritons by computationally modelling the light-harvesting complex 2 (LH2) of the purple bacterium *Rhodopseudomonas acidophila* in a microcavity. I also show the possibility of energy transfer between noninteracting LH2s via coupling to a cavity, providing a potentially new way in which photosynthetic energy transfer pathways could be artificially optimized.

Popular science description

The world around us is a colorful place to behold. Behind this colorful splendor is a fine interplay between light and matter, in which some materials absorb certain wavelengths of light which we perceive as colors that other materials do not. Absorption of light can be properly understood through the framework of quantum mechanics: in an absorption event, a quantum of light – a photon – is absorbed by electrons in a molecule, after which the molecule gains the energy of the absorbed photon. The molecule is then said to be in an excited state. In the case of plants and algae and some microbes that are capable of photosynthesis, the characteristic green hue is caused by special light-absorbing pigments, the chlorophylls. The wavelengths of light that are absorbed by these pigments are crucial for making photosynthesis and consequently most of life on earth possible.

Multiple chlorophyll molecules close to each other can interact as a group, leading to striking changes in the wavelengths of light that are absorbed. In such circumstances it is no longer possible to determine with certainty which of the chlorophylls partake in the absorption event – it is as if all of the chlorophylls act as a single excited entity. Such collective quantum states of matter are called excitons. It turns out that there is a photosynthetic group of bacteria, the purple bacteria, which harness a special light absorbing structure called LH2. The wavelengths that the LH2 absorbs can only be explained using the theory of excitons, giving a hint of the importance of quantum mechanics in biology.

The story does not end with excitons, however. Over the last few years, researchers have become increasingly more interested in investigating the properties of pigments in cavities, that is, between two mirrors. When light of suitable wavelength is shone into the cavity, the light not only excites the molecules in the cavity but also partakes in the excited state itself. Such an excited state, which is partially light and partially matter, is known as a polariton. A polariton is a highly delocalized state, meaning that all of the excited molecules in the cavity are a part of it. It is like a tensed bowstring, which remains tensed by the action of light.

In my thesis, I explore these light-matter states in the case of the LH2 of the purple bacterium *Rhodopseudomonas acidophila*. I explain the observed absorption properties of the LH2 inside a cavity with computational models. I also take a step further and investigate what happens after the excitation of polaritons: how do they finally break down and where does their energy transfer? It is already known that polaritons harness many interesting properties, such as the capability of enhancing chemical reactions. Furthermore, the quantum properties of groups of molecules are known to be enhanced in cavities. In addition to validating more well known properties of polaritons involving LH2s, I show that the delocalized nature of the polaritons enable energy to be transferred between spatially separated LH2s. My thesis might thus offer tools for not only obtaining a clearer understanding on the significance of quantum mechanics in biology, but also for potential applications related to utilizing photosynthesis – perhaps in solar powered technologies of the future.

Acknowledgements

First and foremost, I would like to thank Prof. Tönu Pullerits for guiding me through this fascinating project during the autumn semester. With his broad expertise and the pioneering work he has done in the field of photosynthesis, he has had the ability to introduce me to difficult topics via practical, hands-on steps. Thanks to him, I have become confident in continuing my career as a professional physicist.

The scientist who played an important role in giving me the spark to choose Lund as the place for my master's studies is Daniel Finkelstein Shapiro. He was the first to tell me about the lucrative subject of cavity quantum electrodynamics and its relation to photosynthesis research, which was very important to me for evaluating the prospect of working as a physicist on topics related to photosynthesis in general.

Looking further back, the coordinator of the master's programme, Carl Troein, solidified my choice of changing my major from chemistry to biophysics by describing the importance of mathematical pen and paper based work in biophysical research. Having now done my master's thesis, I can happily say that he was right.

My stay in Lund would have surely been a completely different experience if it wasn't for my wife and the love of my life, Anni, who motivated and cheered me up through the dullest times of the coronavirus pandemic. I would also like to thank everyone else, including my family members, who have supported the academic decisions I have made along the way.

Contents

1 Introduction

Photosynthesis is initiated by absorption of a photon by a light-harvesting complex (LHC), a photosynthetic protein-pigment complex, which then transfers the solar energy to the reaction center [1]. In the reaction center, the primary energy conversion step, charge separation, takes place, and it is the charge separation that drives all the subsequent reactions of photosynthesis, culminating in synthesis of organic compounds [1, 2]. Not only does photosynthesis sustain life on Earth, it has a potential to be utilized in viable, new renewable energy sources of the future [1]. For this reason, thorough understanding of photosynthesis is an important goal not only in fundamental, but also in applied science context.

As a rather new emerging field, cavity quantum electrodynamics extended to biological systems has opened up new ways to study the role of quantum coherence in natural photosynthetic energy transport [3]. In particular, utilizing cavities with modes that are strongly coupled to the photosynthetic organism could provide means to alter the energy transfer pathways within the organism [4]. To this end, optical microcavities have been shown to induce strong coupling in a variety of different systems, including inorganic systems such as quantum dots and semiconductors, but also in organic molecules such as LHCs of green sulfur bacteria [4].

LHCs consist of light-absorbing molecules, or chromophores, typically attached to a protein structure [5]. In most cases, interactions between neighbouring chromophores prevents the excitation of only one chromophore [6]. Instead, the coupling of neighbouring molecules to each other brings about the formation of delocalized energy eigenstates, Frenkel excitons [7]. By definition, a Frenkel exciton constitutes one or more delocalized electron-hole pairs in such a way that for any given pair, the electron and the hole are located in the same molecule [8]. The missing electron in the highest occupied molecular orbital of an excited molecule can then be considered the hole, which together with the electron in the excited electronic state forms the electron-hole pair [8].

Frenkel excitons appear in groups of weakly bound molecules, called aggregates, such as biological chromophore complexes, where the overlap between the electronic wavefunctions of the constituent molecules is negligible [8]; the chromophores involved in a given Frenkel exciton do not have to be in contact with each other in order for the excited state to be delocalized [6]. Frenkel excitons, however, are not the only group of excitons. Charge transfer excitons are induced in cases where the wavefunctions of the molecules overlap more significantly [8] so that the excited electron will be localized in a neighbouring molecule with respect to the hole [9]. On the other side of the spectrum, the electron-hole pair in Wannier-Mott excitons is separated by a much larger distance than the spacing between neighbouring molecules or atoms [8]. Such excitons are often encountered in inorganic semiconductors [9].

The LHC of purple bacteria is know as the light-harvesting complex 2 (LH2), the chromophores of which are bacteriochlorophyll a (Bchl a) molecules. The LH2 of purple bacteria is a protein-pigment complex, which includes two Bchl a ring structures, B800 and B850, which contain 9

and 18 Bchls, respectively. The Bchls in the B800 ring are more widely separated by $\sim$ 2 nm, whereas the short ($\sim$ 0.9 nm) spacing of the Bchls in the B850 ring induces the formation of highly delocalized exciton states. The energies of the excitons in the B850 ring vary from the excited B800 states, so that B800 absorbs light at 800 nm and B850 at around 850 nm. [10, 11]

If the LHC is coupled to a cavity mode, the optical properties of the system can change drastically. The tuning of the cavity is determined by the spacing of the mirrors and the incident angle of the light which is used to excite the LHC [12–14]. The cavity can couple to the molecules strongly, leading to macroscopic coherent states involving hundreds of thousands of excitons [15, 16]. The states also include one or more occupied photonic cavity modes, and are consequently known as polaritons [14–16]. Molecular polaritons thus are characterized by the mixing, or hybridization of the photonic and the molecular states [4, 17]. Because the molecules in the cavity absorb light cooperatively with the cavity mode, new absorption bands, the lower polariton (LP) and upper polariton (UP) branches appear in spectra [14, 15]. Between the LP and UP branches is a branch of states sometimes known as the middle polariton (MP) branch [18]. The states in the MP branch are known as dark states if the molecules in the cavity do not interact with each other [7], because the transitions to these states from the ground state are forbidden [17]. However, the interactions between the Bchl a molecules in the LH2 imply that the visibility, or the absorption intensity of the MP branch has to be evaluated in the case of LH2s in a cavity. Furthermore, the macroscopic coherence of polariton states involving multiple LH2s has not yet been shown.

In this thesis, I will describe how the visibility of polaritons is related to the photon component of the polaritons. Such an approach of determining polaritonic visibility will give rise to the LP, UP and MP absorption branches for isolated LH2s in a cavity within the framework of cavity quantum electrodynamics. I will also show the possibility of exciting multiple noninteracting LH2s via exciting a single polaritonic branch. The delocalized polariton states involving multiple noninteracting photosynthetic units will also open up a door to the possibility of energy transport from one unit to another via the coupling to the cavity alone. Subsequent studies could be applied to whole organisms coupled to a cavity mode, and reveal new ways in which energy could be collected or delivered not only with photosynthetic pigments, but also with optoelectronic materials in general [16, 19].

The structure of this thesis is as follows. In Section 2.1 I describe the theoretical background of excitons and how they relate to the conventional spectrum of the LH2 outside of the cavity. In Sections 2.2-2.4 I extend the theory to the case of the cavity coupled to the LH2, and give precise definitions for the molecular polaritons of different cavity-LH2 systems. In Sections 2.5 and 2.6 I describe a theory of energy transfer with and without the cavity when the LH2s do not interact with each other. Simulations of the models are described in Sections 3 and 4, and finally a discussion followed by a conclusion section are given in Sections 5 and 6.

2 Theory and Background

Photosynthetic light-harvesting complexes act as Frenkel excitons upon excitation by light [8]. Because a Frenkel exciton is a delocalized system of intramolecular electron-hole pairs, it can be expressed as a linear combination of the excited electronic states of the molecules as

$$|\alpha\rangle = \sum_m c_\alpha(m)\,|m\rangle\,. \tag{2.1}$$

Here, $|m\rangle$ is a state in which one or more molecules are excited and the rest are in their ground-states [5, 8], and the factors, $c_\alpha(m)$, are the probability amplitudes of each such excited state. The number of excited molecules corresponds to the number of photons absorbed by the aggregate [8]. In this thesis, the focus is on the more common case where only one of the molecules in the states, $|m\rangle$, is excited. The formation of multiply excited states requires very high light intensities, which increases the probability of multiple photons hitting a single chromophore nearly simultaneously [20]. Double excitations can also be induced by two near simultaneous laser pulses as in time-resolved spectroscopy techniques [21]. In the case of single excitations, the number of the states, $|m\rangle$, corresponds to the number of molecules in the aggregate, and it is convenient to denote the index, m, as the index of the excited molecule in question. Consequently, the states $|m\rangle$ are commonly known as the site basis states [6, 22]. Because a Frenkel exciton forms upon electronic excitation of a chromophore aggregate, it is an eigenstate of the electronic Hamiltonian [5]. In order to find the energies and the probability amplitudes, $c_\alpha(m)$, characterizing the excitonic states, the electronic Schrödinger equation for the system in question in the basis of the singly excited molecular states has to be solved.

2.1 The Hamiltonian of Frenkel Excitons

The Hamiltonian of a molecular aggregate consisting of N_m molecules is given as

$$\hat{H}_{agg} = \sum_m \hat{H}_m + \frac{1}{2}\sum_m \sum_{n\neq m} \hat{V}_{mn}, \tag{2.2}$$

where $\hat{H}_m$ are the Hamiltonians for each individual molecule labelled with m, and where $\hat{V}_{mn}$ are the potential energy operators between the molecules m and n. The intramolecular Hamiltonians include the kinetic and potential energies of the nuclei and the electrons in each molecule, whereas the intermolecular potentials include the Coulomb interactions between the molecules. [8]

One can assume that the dimensions of the molecules are negligible compared to the intermolecular separations. Using such an approximation simplifies the contribution of the operators $\hat{V}_{mn}$ in the site basis $\{|k\rangle\}$, so that the interactions between the molecules upon excitation

become interactions between molecular point dipoles, leading to an approximation known as the dipole-dipole approximation. With the dipole-dipole approximation, one arrives at the electronic Hamiltonian of Frenkel excitons,

$$\hat{H} = \sum_k E_k \left|k\right\rangle \left\langle k\right| + \sum_l \sum_{k \neq l} V_{kl} \left|k\right\rangle \left\langle l\right| . \tag{2.3}$$

The orthonormal site basis states $|k\rangle$ are of the form

$$\left|k\right\rangle = \left|e(k)\right\rangle \prod_{k' \neq k} \left|g(k')\right\rangle , \tag{2.4}$$

where $|e(k)\rangle$ and $|g(k')\rangle$ are the excited and ground states of the molecules k and k', respectively. The energies E_k, also known as the site energies [6], are the energies of the excited chlorophylls k, whereas the interactions between the point dipoles are

$$V_{kl} = \frac{1}{4\pi\epsilon}\{\frac{\boldsymbol{\mu}_k \cdot \boldsymbol{\mu}_l^*}{|\mathbf{x}_{kl}|^3} + 3\frac{(\boldsymbol{\mu}_k \cdot \mathbf{x}_{kl})(\boldsymbol{\mu}_l^* \cdot \mathbf{x}_{kl})}{|\mathbf{x}_{kl}|^5}\}, \tag{2.5}$$

where $\mathbf{x}_{kl}$ is the position vector from the center of mass of the molecule k to the center of mass of the molecule l, ϵ is the permittivity of the medium and $\boldsymbol{\mu}_k$ is known as the transition dipole moment of the molecule k,

$$\boldsymbol{\mu}_k = \left\langle e(k)\right|\hat{\boldsymbol{\mu}}_k\left|g(k)\right\rangle , \tag{2.6}$$

with the relevant dipole moment operator

$$\hat{\boldsymbol{\mu}}_k = -e \sum_{i \in k} \hat{\mathbf{r}}_{ik}. \tag{2.7}$$

The summation refers to all of the electrons in the molecule k with the electronic position operators $\hat{\mathbf{r}}_{ik}$. [6, 8]

From Eq. 2.5 it follows that $V_{kl}^* = V_{lk}$, so H has to be Hermitian. Specifically, if the molecular wavefunctions are real-valued, the matrix of the Hamiltonian will be a real and symmetric. Without loss of generality, $(\psi_a + \psi_a^*)/2 = \mathrm{Re}(\psi_a)$ or $(\psi_a - \psi_a^*)/2i = \mathrm{Im}(\psi_a)$ can always be chosen to be the solution to the Schrödinger equation with the same eigenvalue as ψ_a [23]. Hence, I will assume real-valued wavefunctions, transition dipole moments and matrix elements of the Hamiltonian in the following sections.

The absorption intensity for a given transition depends on the square of the transition dipole moment of the exciton [19, 24]. The ground state of the aggregate is the product state in which all of the chlorophylls are in their ground states. Thus, the transition dipole moment of a transition from the ground state to the excitonic state given by Eq. 2.1 is

$$\boldsymbol{\mu}_\alpha = \left\langle \alpha\right|\hat{\boldsymbol{\mu}}\left|g\right\rangle = \sum_m c_\alpha(m) \left\langle m\right|\hat{\boldsymbol{\mu}}\left|g\right\rangle , \tag{2.8}$$

where $\hat{\boldsymbol{\mu}}$ is the dipole moment operator of all the chlorophylls,

$$\hat{\boldsymbol{\mu}} = \sum_n \hat{\boldsymbol{\mu}}_n. \tag{2.9}$$

The terms $\langle m|\boldsymbol{\mu}_n|g\rangle$ with $n \neq m$ obey

$$\langle m|\hat{\boldsymbol{\mu}}_n|g\rangle = \langle g(n)|\hat{\boldsymbol{\mu}}_n|g(n)\rangle \langle e(m)|g(m)\rangle \prod_{i\neq m,n} \langle g(i)|g(i)\rangle = 0, \tag{2.10}$$

which reduces Eq. 2.8 into

$$\boldsymbol{\mu}_\alpha = \sum_m c_\alpha(m) \langle e(m)|\hat{\boldsymbol{\mu}}_m|g(m)\rangle = \sum_m c_\alpha(m)\boldsymbol{\mu}_m. \tag{2.11}$$

The absorption intensity of the excitonic transition should thus obey the dependence

$$A_\alpha \sim |\boldsymbol{\mu}_\alpha|^2. \tag{2.12}$$

Furthermore, each absorption peak of a given $|G\rangle \rightarrow |\alpha\rangle$ transition should be broadened due their finite lifetime [25] and to the coupling of the electronic transitions to the nuclear motions of the system and the surroundings [8, 20]. [8]

2.2 Hamiltonian of an LH2-cavity polariton

The Hamiltonian of a chlorophyll-protein complex affected by light includes the system (S) of chlorophylls in the complex, vibrational reservoir (R) and light (L), and is given as

$$H = H_S + H_{S-R} + H_R + H_{S-L} + H_L \tag{2.13}$$

[26] [27]. The Hamiltonian of the chlorophylls, H_S, can be written as the Frenkel exciton Hamiltonian, whereas the reservoir with the Hamiltonian H_R represents the vibrational normal modes of the system, or the intra-pigment vibrations and the vibrational motion of the protein and the solvent [26]. The reservoir plays a role in describing the energy transfer dynamics after an excitation event [26, 28]. One can approximate the contribution of H_{S-R} to the electronic system explicitly as small diagonal disorder elements, δE_n, so that the site energies will be transformed as $E_n \rightarrow E_n + \delta E_n$ [22]. This represents the variations in the local electrostatics environments of each chlorophyll [26], and explicitly accounts for the broadening of absorption peaks (Section 2.1). Assuming identical pigments, E_n can be written as a constant energy, E, for all n. The time-dependent behaviour of H_{S-R} also induces transfer between excited electronic states, which will be explored more thoroughly later in this thesis.

The eigenstates of the photonic Hamiltonian, H_L, of a given cavity mode can be expressed as the number states, $|n\rangle$, where n is the number of photons occupying the cavity mode [27,

29]. The corresponding photon energies are $E_n = (n + \frac{1}{2})\hbar\omega$, where ω is the frequency of the cavity mode [27, 29]. Only the energy difference between transitions dictates which wavelength will be absorbed, so it is convenient to set the ground state energy of the cavity mode and the chlorophylls to zero. Due to the finite time the photons occupy the cavity, the energy of the cavity is broadened. It is possible to take this cavity broadening into account already when constructing the Hamiltonian [18], but I will take a simpler approach and completely characterize the cavity with only a single mode. The frequency of this mode can be determined with Maxwell's equations for a beam of monochromatic light that hits the cavity at an incident angle, θ, giving

$$\omega = \frac{c}{n_r}\sqrt{\frac{\pi^2}{d^2} + \frac{2\pi}{\lambda}\sin\theta}, \tag{2.14}$$

where n_r is the refractive index of the medium inside the cavity, c is the speed of light, d is the cavity width and λ is the wavelength of the incident light [12–14]. The corresponding wavelength supported by the cavity mode is $\lambda_{cavity} = 2\pi c/\omega n_r$.

As a thought experiment, one can start with an LH2 inside a cavity but in the absence of photons. The system will be in the ground state state $|n = 0, G\rangle$, where $|G\rangle$ refers to the molecular ground state and $|n = 0\rangle$ to the number state of the unoccupied cavity mode [18]. Exciting the LH2 requires using photons of energy close to, but not necessarily equal to the energy difference between the excited and the ground state of the LH2 [30]. As photons having such energies enter the cavity, the system will initially be in the state $|n = N_c, G\rangle$. If one of the photons excites the LH2 from the ground state to an arbitrary excited state $|k\rangle$, the system will be in the state $|n = N_c - 1, k\rangle$, where the molecule k is excited. Because quantum mechanics is a probabilistic theory, there is a specific probability amplitude that characterizes the excited state $|n = N_c - 1, k\rangle$. As any of the molecules can become excited, a suitable state to represent the LH2 inside the cavity with photons is thus a superposition of the states $|n = N_c, G\rangle$ and $|n = N_c - 1, k\rangle$.

Using the notation $|N_c, G\rangle$ and $|N_c - 1, k\rangle$ for the orthonormal states $|n = N_c, G\rangle$ and $|n = N_c - 1, k\rangle$, respectively, the Hamiltonian of the LH2-cavity polariton is

$$\begin{aligned} H = \hbar\omega\,|N_c, G\rangle\langle N_c, G| + \sum_k J_{1,k}\,|N_c, G\rangle\langle N_c - 1, k| \\ + \sum_k J_{k,1}\,|N_c - 1, k\rangle\langle N_c, G| + \sum_{k\neq l} V_{kl}\,|N_c - 1, k\rangle\langle N_c - 1, l| \\ + \sum_k E_k\,|N_c - 1, k\rangle\langle N_c - 1, k|\,, \end{aligned} \tag{2.15}$$

where $\hbar\omega$ is the energy of a photon in the cavity mode, and the last two terms correspond to the Frenkel exciton Hamiltonian of Eq. 2.3. As written for example in [18] and [19], the matrix element $\langle N_c, G|H|N_c, G\rangle$ corresponds to the energy of a single photon, $\hbar\omega$, instead of $N_c\hbar\omega$. This can be understood by regarding the state $|N_c - 1, G\rangle$ as the initial state before excitation, so that the spectroscopically relevant energy of the photons is then the energy

difference between the polariton and $|N_c - 1, G\rangle$: $N_c\hbar\omega - (N_c - 1)\hbar\omega = \hbar\omega$. The number states $|N_c - 1\rangle$ do not affect the couplings V_{kl}, which thus can be taken as the couplings of the point dipole chlorophylls.

The couplings $J_{1,k}$ and $J_{k,1}$ are due to the coupling of the electromagnetic field to the transition dipole moments of the chlorophylls via the system-light interaction H_{S-L}. The electric field with a wavelength of ~ 800 nm does not vary much over a single LH2 complex [11], allowing the light-matter interaction to be approximated as

$$H_{S-L} = -\hat{\mathbf{E}}(\mathbf{X}_0) \cdot \hat{\boldsymbol{\mu}}(\mathbf{r}), \tag{2.16}$$

where $\hat{\mathbf{E}}(\mathbf{X}_0)$ is the electric field operator evaluated at the center of mass of the LH2, and where $\hat{\boldsymbol{\mu}}(\mathbf{r})$ is the dipole-moment operator of the electrons,

$$\hat{\boldsymbol{\mu}}(\mathbf{r}) = -e\sum_i \hat{\mathbf{r}}_i \tag{2.17}$$

[8, 29, 31]. The field operator $\hat{\mathbf{E}}$ is a function of the photon annihilation and creation operators, $\hat{a}$ and $\hat{a}^\dagger$, respectively, which operate the relevant number states as $\hat{a}\,|N_c\rangle = \sqrt{N_c}\,|N_c - 1\rangle$ and $\hat{a}^\dagger\,|N_c - 1\rangle = \sqrt{N_c}\,|N_c\rangle$ [29]. Working with the dipole moment operator in a similar way as in Section 2.1 and setting the origin to $\mathbf{X}_0$, the matrix elements $J_{1,k}$ and $J_{k,1}$ obtain the form

$$J_{1,k} = J_{k,1} = -E\cos(\theta_k)|\boldsymbol{\mu}_k| = -E\mu_{k,x_i}, \tag{2.18}$$

where the angle θ_k is the angle between the polarization of the cavity mode and the molecular transition dipole moment, μ_{k,x_i} is the component of $\boldsymbol{\mu}_k$ in the direction of the polarization of the cavity mode and the scalar E has the dimensions of an electric field and depends on the square root of the number of photons and the number of molecules, $\sqrt{N_c}$ and $\sqrt{N_m}$, respectively. The scalar E also depends on the inverse of the square root of the volume of the cavity, which favours strong coupling in small microcavities. Strong coupling is a requirement for the formation of true polaritons with part molecular and part light character, which I will show later in this thesis. Hence, cavities with large volumes do not support the formation of polaritons. For brevity, I will refer to using Eq. 2.18 as calculating the polariton in the molecular picture. For more details, see [8, 12, 18, 29, 31–35].

In a population of randomly oriented LH2s, the orientations of the transition dipole moments vary from one LH2 to another. As will be justified later in this thesis, most of the differently directed LH2s likely contribute to the absorption spectrum roughly similarly. Hence, I assume that for each k, there exists some value $\overline{\cos(\theta_k)}$ that correctly predicts the averaged contribution of multiple differently oriented LH2s to the spectrum. For a population of LH2s, the correct form of the matrix elements is then

$$J_{1,k} = J_{k,1} = E\overline{\cos(\theta_k)}|\boldsymbol{\mu}_k|. \tag{2.19}$$

For convenience, I have included the negative sign in Eq. 2.18 to the expression of $\overline{\cos(\theta_k)}$. The contribution of an arbitrary chlorophyll to the energy of the polariton due to coupling

with the field does not depend on the location of the chlorophyll within the LH2, but only on the direction of its transition dipole moment. Consequently, if the chlorophylls interact with the electric field independently of each other, the averages $\overline{\cos(\theta_k)}$ in Eq. 2.19 in a randomly oriented population of LH2s will be the same for all k.

The eigenstates of the Hamiltonian given in Eq. 2.15 are known as polaritons [12, 32]. To simplify notation, I will use $N_c = 1_c$ for the remainder of the thesis. The polariton states will then be of the form

$$|J\rangle = c_J(0)\,|1_c, G\rangle + \sum_m c_J(m)\,|0_c, m\rangle\,. \tag{2.20}$$

The squares of the constants $c_J(0)$ and $c_J(m)$ are called the Hopfield, or mixing coefficients, and represent the optical and material character of the polariton, respectively [4, 12]. Consequently, I refer to $|c_J(0)|^2$ as the photonic and $|c_J(m)|^2$ as the molecular Hopfield constants of the polariton state $|J\rangle$. As implied by [14] and [36], the visibility of a polariton is determined by the photonic Hopfield coefficient, $|c_J(0)|^2$:

$$A_J \sim |c_J(0)|^2. \tag{2.21}$$

I will also follow this practice in this thesis, and neglect any dependence of A_J on the molecular transition dipole moments.

An intuitive way to understand the visibility relation 2.21 is as follows. For a polariton to become excited, a photon of suitable energy must first get inside the cavity. This is possible as long as the photonic Hopfield coefficient of the polariton is non-zero. Inside the cavity, the photon automatically becomes coupled to the molecules via the polaritonic Hamiltonian given in Eq. 2.15, and no further dependence of the transition intensity on the transition dipole moments is needed. In other words, the dipole moments of the molecules indirectly affect the transition intensity via the photonic Hopfield coefficient, which depends on the eigenstates of the Hamiltonian. One can hence think of the light outside the cavity as interacting only with the cavity mode and thus with the polariton via the Hopfield coefficient and regard the light inside the cavity as interacting with the molecules as separate entities. The notion of absorbance when $|c_J(0)|^2 \approx 1$, however, is difficult to understand. Perhaps the relation 2.21 is not complete and should be complemented with some factor that depends on the molecular transition dipole moments. An intuitive modification of the relation 2.21 would be to multiply the photonic Hopfield coefficient with the square of the transition dipole moment of the molecular part of the polariton. I do not investigate such an approach in this thesis.

The multiple eigenstates of the polaritonic Hamiltonian all have different energies. In order to excite a polariton, the photons that hit the cavity have to match the energy of one of these polaritons. The frequency of the cavity in Eq. 2.15, however, is fixed, and differs from the energy of the polaritons. This is not a contradiction, because if a photon of suitable energy excites a polariton, the photon will afterwards be involved in the polariton state (Eq. 2.20), since the occupied cavity mode is a part of the polariton. In this way, energy conservation is obeyed.

2.3 Coupling the cavity mode to the excitonic states

I have previously described how excitons arise from the collective interactions of the transition dipole moments of the molecules. One can also make an assumption that the cavity field does not interact with the individual molecular dipole moments independently, but instead interacts with the dipole moment of the excitons as given by Eq. 2.11. When coupling the cavity mode to the excitons, one has to use the basis $\{|1_c, G\rangle, |0_c, \alpha\rangle\}$, where $|\alpha\rangle$ are the 27 different exciton states of LH2 and $|1_c, G\rangle$ is the photonic state. In this basis, the Hamiltonian will be

$$\begin{aligned} H = \hbar\omega \left|1_c, G\right\rangle \left\langle 1_c, G\right| + \sum_\alpha J_{1,\alpha} \left|1_c, G\right\rangle \left\langle 0_c, \alpha\right| \\ + \sum_\alpha J_{\alpha,1} \left|0_c, \alpha\right\rangle \left\langle 1_c, G\right| + \sum_\alpha E_\alpha \left|0_c, \alpha\right\rangle \left\langle 0_c, \alpha\right|, \end{aligned} \tag{2.22}$$

where E_α is the energy of the exciton $|\alpha\rangle$.

Within a given LH2, the relative directions of the molecular transition dipole moments, $\boldsymbol{\mu}_m$, depend on the orientation of the LH2 complex in the laboratory frame (Fig. 1 **c**). Assuming that the cavity mode supports a wavelength (cf. Eq. 2.14) that is very long compared to the size of an LH2 complex so that the cavity interacts with whole LH2 units via excitons instead of individual, independent chlorophylls, the couplings to the field in a population of LH2s will be given as

$$J_{1,\alpha} = E' |\boldsymbol{\mu}_\alpha|, \tag{2.23}$$

where E' is the coupling constant including any dependence on the directionality of the polarization and $\boldsymbol{\mu}_\alpha$ is the transition dipole moment of the exciton as given by Eq. 2.11. Eq. 2.23 implies that on average, the angle between the polarization and the excitonic transition dipole moment is the same for each exciton. Such an assumption can be understood by noting that in a population of randomly oriented LH2s, no direction is inherently favoured over the other so the contribution of an arbitrary exciton to the energy of the system only depends on the magnitude of the transition dipole moment of the exciton state $|\alpha\rangle$. I will refer to calculating the polaritons with Eq. 2.23 as using the excitonic picture.

If the picture of independent excitons is correct, the terms $\overline{\cos(\theta_k)}$ given in Eq. 2.19 can be obtained via a change of basis from excitons to the site basis:

$$\sum_\alpha J_{1,\alpha} \left|1_c, G\right\rangle \left\langle 0_c, \alpha\right| = \sum_\alpha \sum_k c_\alpha(k) J_{1,\alpha} \left|1_c, G\right\rangle \left\langle 0_c, k\right|. \tag{2.24}$$

Comparing Eq. 2.24 with Eq. 2.15 and 2.19 gives

$$J_{1,k} = \sum_\alpha c_\alpha(k) J_{1,\alpha} = E' \sum_\alpha c_\alpha(k) |\boldsymbol{\mu}_\alpha| = E |\boldsymbol{\mu}_k| \overline{\cos(\theta_k)}. \tag{2.25}$$

Assuming the equality $E = E'$, it then follows that

$$\overline{\cos(\theta_k)} = \frac{\sum_\alpha c_\alpha(k) |\boldsymbol{\mu}_\alpha|}{|\boldsymbol{\mu}_k|}. \tag{2.26}$$

Any difference between the constants E and E' will be included in the expressions of $\overline{\cos(\theta_m)}$; the assumption $E = E'$ will always give the correct form of the coefficients $J_{1,k}$ after the change of basis. For the rest of this thesis, $E = E'$ is always assumed.

The eigenstates of the Hamiltonian given in Eq. 2.22 are the polariton states of the form

$$|J\rangle = c_J(0)\,|1_c, G\rangle + \sum_{\alpha} c_J(\alpha)\,|0_c, \alpha\rangle\,, \tag{2.27}$$

where the excitonic basis is used instead of the site basis. I refer to the corresponding Hopfield constants as the photonic and excitonic Hopfield coefficients. As with the molecular picture, the absorption signals of the polaritons expressed in the excitonic picture can also be expected to obey the relation 2.21. In this thesis, I refer to polaritons calculated both in the molecular and excitonic picture simply as molecular polaritons.

2.4 Polaritonic Hamiltonian of two noninteracting LH2s

The Hamiltonian of two LH2s or two groups of LH2s can be formed by using either the molecular or the excitonic basis. In the site basis, extra states $|0_c, k\rangle$ have to be used for the molecules in the other LH2, whereas with the excitonic basis, extra states $|0_c, \alpha\rangle$ that are formed from the excitons in the other LH2 have to be used. Due to the fluctuations of the local environments of the bacteriochlorophylls, diagonal disorders δE_n to the energies of each chlorophyll n in both LH2s have to be included (cf. Section 2.2). The only difference between the matrix elements corresponding to the two LH2s comes then from the use of different diagonal disorders in the chlorophyll sites of the two LH2s (Appendix A). The couplings between the second LH2 and the cavity are consequently also different.

In this thesis, I assume no direct interactions between the two LH2s, meaning that the matrix elements $\langle a|H|b\rangle$, where $|a\rangle$ includes the site state or the exciton of one LH2 and $|b\rangle$ the site state or the exciton of the other, are zero. Any significant differences between the simulations with one or two LH2s are thus due to the coupling to the cavity. In order to keep the coupling strength at a similar magnitude, the coupling constants E' and E can be assumed to be unchanged. One can justify such an assumption by either regarding the two LH2s as being two groups of LH2s characterized by different disorders or as being a part of a bigger group of LH2s. The same can be said when applying the excitonic picture to the couplings.

2.5 Relaxation of excitons

After a light absorption event, an exciton of an LH2 is excited. Such a situation is clearly far from a thermodynamic equilibrium. Energy will then start to transfer from the exciton to the surrounding environment and vice versa, until a thermodynamic equilibrium is again reached.

An important factor for this relaxation of excited electronic states is coupling to the vibrational degrees of freedom of the surrounding environment, also known as the heat bath. A relaxation process via vibrational coupling can be understood within the framework of a model termed as the surface hopping model. [8]

In the surface hopping model, the electronic eigenstates are regarded as potential energy surfaces, which are solved adiabatically as a function of the nuclear coordinates, $\mathbf{R}$. The evolution of the electronic system, however, is affected by the time-dependent change of the nuclear coordinates. Thus, the time-dependent Schrödinger equation of the electrons,

$$i\hbar\frac{\partial}{\partial t}\Psi(\mathbf{r},\mathbf{R}(t),t) = (H_S + H_{S-R}(\mathbf{r},\mathbf{R}(t)))\Psi(\mathbf{r},\mathbf{R}(t),t), \tag{2.28}$$

is to be solved non-adiabatically by taking the time-dependent behaviour of the nuclear coordinates into account. The hops, or transfers from one electronic state or adiabatic surface to another occurs thus via the system-bath coupling, $H_{S-R}(\mathbf{r},\mathbf{R}(t))$. As with the coupling between electrons and an external electromagnetic field, a transfer can occur if the energy of the interacting phonons is close to resonance of the energy difference between the initial and final electronic states. However, if the density of phonons is negligible at levels corresponding to the electronic energy difference, surface hopping will essentially not occur. In the following discussion, this density is given by the product $D(E)n(E,T)$, where $D(E)$ is the density of states and $n(E,T)$ the Bose-Einstein distribution of the phonons at energy E and at temperature T. The coupling strength itself has to also be nonzero, which in the following discussion is given by a factor j_0. [8]

A complete quantum description of the relaxation process can be formulated by utilizing the theory of open quantum systems. By definition, a quantum system that can exchange energy with the surroundings is an open quantum system [37]. In the case of LH2, the environment can be regarded as the nuclei of the chlorophylls and the protein in which the photosynthetic pigments are embedded [6], and energy is exchanged with the vibrational normal modes of the environment [28]. The open system is the chlorophyll rings of multiple LH2s, each of which can be in different electronic states. The vibrational states of the proteins of LH2s can also differ from one LH2-complex to another. It is nevertheless possible to deal with the different electronic and vibrational states of the LH2s statistically and derive equations of motion for the different populations of the electronic states of the LH2 [38]. Let p_α be the population of the exciton $|\alpha\rangle$. The equations of motion are then

$$\dot{p}_\alpha = \sum_\beta (W_{\beta\alpha}p_\beta - W_{\alpha\beta}p_\alpha) - \frac{p_\alpha}{\tau_{exc}}, \tag{2.29}$$

where $W_{\beta\alpha}$ is the exciton transfer rate from the state $|\beta\rangle$ to $|\alpha\rangle$ and τ_{exc} is the lifetime of the exciton $|\alpha\rangle$ before decaying to the ground state [28]. An $\alpha \to \alpha$ type transfer does not occur, so $W_{\alpha\beta} = 0$ for $\alpha = \beta$.

Two processes that play an important role in driving the decay to the ground state are internal conversion (IC) and fluorescence. Internal conversion is due to the same physical principles

as the surface hopping between excited states [8, 20], whereas in fluorescence, the molecular unit loses its excitation energy via a concurrent, spontaneous emission of a photon [20]. Eq. 2.29 without the transfer to the ground state is referred to as the Pauli master equation [8, 38]. The Pauli master equation with the rate constants $W_{\alpha\beta}$ involves transfers that are due to the coupling to the vibrational modes of the bath, whereas the decay to the ground state is due to other processes, such as spontaneous emission. Assuming that the phonon bath is large enough to remain in thermal equilibrium thorough the relaxation process, only a negligible fraction of the phonons will have energies corresponding to the transition between the ground and first excited electronic states. Thus, transfers between the exciton and the ground state via vibrational coupling can be ignored.

The vibrational quanta of energy of the bath are phonons, which in thermal equilibrium obey the Bose-Einstein distribution,

$$n(E,T) = \frac{1}{\exp(E/k_B T) - 1}, \tag{2.30}$$

where k_B is the Boltzmann constant, E is the phonon energy and T is temperature [39]. The density of states of the phonon modes also vary with energy. A form of the density of phonon states that has been used successfully in recreating experimental results in LH2 studies is of the form

$$D(E) = \frac{E^2}{E_0^3} \exp(-\frac{E}{E_0}), \tag{2.31}$$

where the parameter E_0 determines the shape of the distribution. With the help of Redfield theory, the rates can then be written as

$$W_{\alpha\beta} = \begin{cases} \frac{2\pi}{\hbar}(1 + n(E_{\alpha\beta}, T))J(E_{\alpha\beta}) \sum_n |c_\alpha(n)|^2 |c_\beta(n)|^2, & E_{\alpha\beta} > 0 \\ \frac{2\pi}{\hbar} n(-E_{\alpha\beta}, T))J(-E_{\alpha\beta}) \sum_n |c_\alpha(n)|^2 |c_\beta(n)|^2, & E_{\alpha\beta} < 0, \end{cases} \tag{2.32}$$

where the energy difference between the excitons is $E_{\alpha\beta} = E_\alpha - E_\beta$, the expansion coefficients $c_\alpha(n)$ of the exciton α are given in Eq. 2.1 and $J(E_{\alpha\beta})$ is the spectral density of the phonons,

$$J(E_{\alpha\beta}) = j_0 D(E_{\alpha\beta}). \tag{2.33}$$

The amplitude j_0 depends on the coupling strength between the system and the bath. [8, 28, 40]

It is intuitive that the rate depends on the number density of phonons with energy $|E_{\alpha,\beta}|$ via the product $n(|E_{\alpha,\beta}|, T)J(|E_{\alpha,\beta}|)$. The rate towards lower energies, however, is faster. The difference in the magnitude of the rates towards states of higher or lower energy can be understood by first observing that without the decay to the ground state, the solution to the system of equations 2.29 predicts with $\dot{p}_\alpha = 0$ the relation

$$p_\alpha = \frac{W_{\beta\alpha}}{W_{\alpha\beta}} p_\beta \tag{2.34}$$

[38]. Without loss of generality, let now $E_{\alpha,\beta} < 0$. Using Eq. 2.32 and noting that $J(-E_{\alpha,\beta}) = J(E_{\beta,\alpha})$, one arrives at the principle of detailed balance,

$$p_\alpha = \frac{W_{\beta\alpha}}{W_{\alpha\beta}} p_\beta = \frac{1 + n(E_{\beta,\alpha}, T)}{n(-E_{\alpha,\beta}, T))} p_\beta = e^{-E_{\alpha,\beta}/k_B T} p_\beta \tag{2.35}$$

[8, 38]. As is stated in [38] and motivated in [41], this implies that in equilibrium, the system obeys Boltzmann statistics with

$$p_\alpha = \frac{e^{-E_\alpha/k_B T}}{Z}, \tag{2.36}$$

where Z is the partition function, which does *not* include the electronic ground state. The Boltzmann distribution arises because of the constant number of LH2s, so that only energy can be exchanged between the system and the environment; a canonical ensemble describes the thermodynamics of the system [39]. Consequently, the relaxation eventually causes states with the lowest energies to be mostly populated (cf. Section 2.5).

The system of equations of motion given by Eq. 2.29 can be cast in a matrix form,

$$\dot{\mathbf{p}} = \mathsf{R}\mathbf{p}, \tag{2.37}$$

where

$$\mathsf{R} = \begin{pmatrix} -\sum_\beta W_{1\beta} - 1/\tau_{exc} & W_{21} & W_{31} & \cdots \\ W_{12} & -\sum_\beta W_{2\beta} - 1/\tau_{exc} & W_{13} & \cdots \\ \cdots & & & \end{pmatrix}. \tag{2.38}$$

The solution is then given as

$$\mathbf{p}(t) = \sum_i c_i e^{\lambda_i t} \mathbf{u}_i, \tag{2.39}$$

where $\mathbf{u}_i$ and λ_i are the eigenvectors and corresponding eigenvalues of the matrix R [42]. Assuming that the eigenvectors are linearly independent as in the case of real-valued and distinct eigenvalues [42], the coefficients c_i can be solved from the initial value problem,

$$\mathbf{p}(0) = \sum_i c_i \mathbf{u}_i. \tag{2.40}$$

Let the matrix U be such that $U_{ij} = [\mathbf{u}_i]_j$, and let the vector $\mathbf{c}$ contain the coefficients c_i. The solution for the coefficients is then

$$\mathbf{c} = \mathsf{U}^{-1}\mathbf{p}(0). \tag{2.41}$$

2.6 Relaxation of polaritons

In order to simulate polaritonic relaxation, a few changes have to be introduced to the excitonic relaxation model. First of all, the rate constants $W_{\alpha\beta}$ have to be replaced by rate constants $W_{JJ'}$

for transfer between polaritons $|J\rangle$ and $|J'\rangle$. Interaction between cavity photon and phonons can be neglected, because the energy of the photon is far from the vibrational levels that are significantly populated. Hence, the rate constants $W_{JJ'}$ cannot depend on the photonic Hopfield coefficients, $|c_J(0)|^2$ via the surface hopping model. As for the sum $\sum_n |c_\alpha(n)|^2|c_\beta(n)|^2$ in Eq. 2.32, the easiest way to carry out the simulation is construct the polaritonic Hamiltonian with the site basis so that the coefficients $c_\alpha(n)$ can simply be replaced by the polaritonic counterparts, $c_J(n)$.

Because the heat bath does not interact with the field, the decay to the ground state for each polariton due to internal conversion and fluorescence will be slower by an amount that depends on the photonic Hopfield coefficient. On the other hand, the photonic component of the polariton can be presumed to undergo a decay due to the cavity lifetime. As done in [20], the decay rate can thus be assumed to be the sum of the rates due to IC and cavity lifetime. Instead of $1/\tau_{exc}$, the decay rate constant of polariton $|J\rangle$ can hence be written as

$$1/\tau(J) = |c_J(0)|^2 \frac{1}{\tau_{cavity}} + \sum_n |c_J(n)|^2 \frac{1}{\tau_{exc}}, \tag{2.42}$$

where $|c_J(0)|^2$ and $|c_J(\alpha)|^2$ are the photonic and molecular Hopfield coefficients, respectively. It is known that the rate of fluorescence can change in a cavity [27], which consequently can change τ_{exc}. For simplicity, I will regardless assume that τ_{exc} remains unaltered in a cavity.

If the medium within the cavity does not affect the speed of light, the cavity lifetime can be written as

$$\tau_{cavity} = \frac{nd}{c(1-R)}, \tag{2.43}$$

where n is the average number of times a photon is refected inside a cavity, d is the distance between the mirrors of the cavity, c is the speed of light and R the reflectivity of the mirrors [27]. Assuming a reflectivity of 0.8, a photon bounces on average 4 times in the cavity before exiting. Assuming $d = 300$ nm, the cavity lifetime is then on the order of 20 fs. Such a fast decay due to the cavity would cause polaritons with even a moderate photonic character to decay essentially instantaneously to the ground state before any relaxation to the other states can occur. However, in a system of thousands of LH2s, there will presumably be many more dark states with close to zero photonic Hopfield coefficients than true polariton states [15]. These states correspond to the states of the LH2 outside of the cavity (cf. dark states in Fig. 6), and likely contribute to an even faster relaxation away from the true polariton states before the cavity decay. One can thus assume that the relaxation from an excited polariton to these dark states has already taken place, and start the simulation from one of the dark states.

3 Simulations involving excitons in the LH2

3.1 Reconstruction of the spectrum of the LH2

The absorption spectrum of the LH2 of the purple bacterium *Rhodopseudomonas acidophila* was constructed from the numerically obtained eigenvalues and eigenstates of the matrix representation of the Frenkel exciton Hamiltonian (Eq. 2.3). Without accounting for the diagonal disorders (cf. Section 2.2), the diagonal terms of the Hamiltonian were set to 12500 cm^{-1} energy equivalent units of wavenumbers, $1/\lambda$ [25], with the corresponding wavelength of $\lambda =$ 800 nm. This value matches the absorption of the B800 chlorophylls, which are known to absorb rather independently of each other [11]. Diagonal disorders were also included via a Gaussian distribution centered on 0 with a variance of 60 and 100 cm^{-1} for the B800 and B850 chlorophylls, respectively (see Appendix A). The disorders slightly broadened the spectrum by splitting the energies of such states that were otherwise degenerate (not shown). Unless otherwise specified, the same diagonal disorders have also been used in the other computations presented in this thesis.

The off-diagonal elements V_{kl} specified by Eq. 2.5 and further evaluated in [8, 43] were provided by Tönu Pullerits from the Department of Chemical Physics, Lund. The positions of the center of masses of the chlorophyll units were set to the positions of the heavy Mg atoms in the center of the chlorophyll molecules by referring to the atomistic structure of the LH2 of the purple bacterium *Rhodopseudomonas acidophila* [11] (Fig. 1 **c**). The directions of the transition dipole moments corresponding to transitions from the ground state to the lowest unoccupied state (LUMO) were specified as in [44]. The partial LH2 spectra were computed by using only the B800 or B850 chlorophylls (Fig. 1 **a**-**b**) and the complete LH2 spectrum was computed with all of the chlorophylls together with the couplings between the B800 and B850 chlorophylls (Fig. 1 **d**). The relative absorption intensity of each eigenstate was obtained with the formulae 2.11 and 2.12.

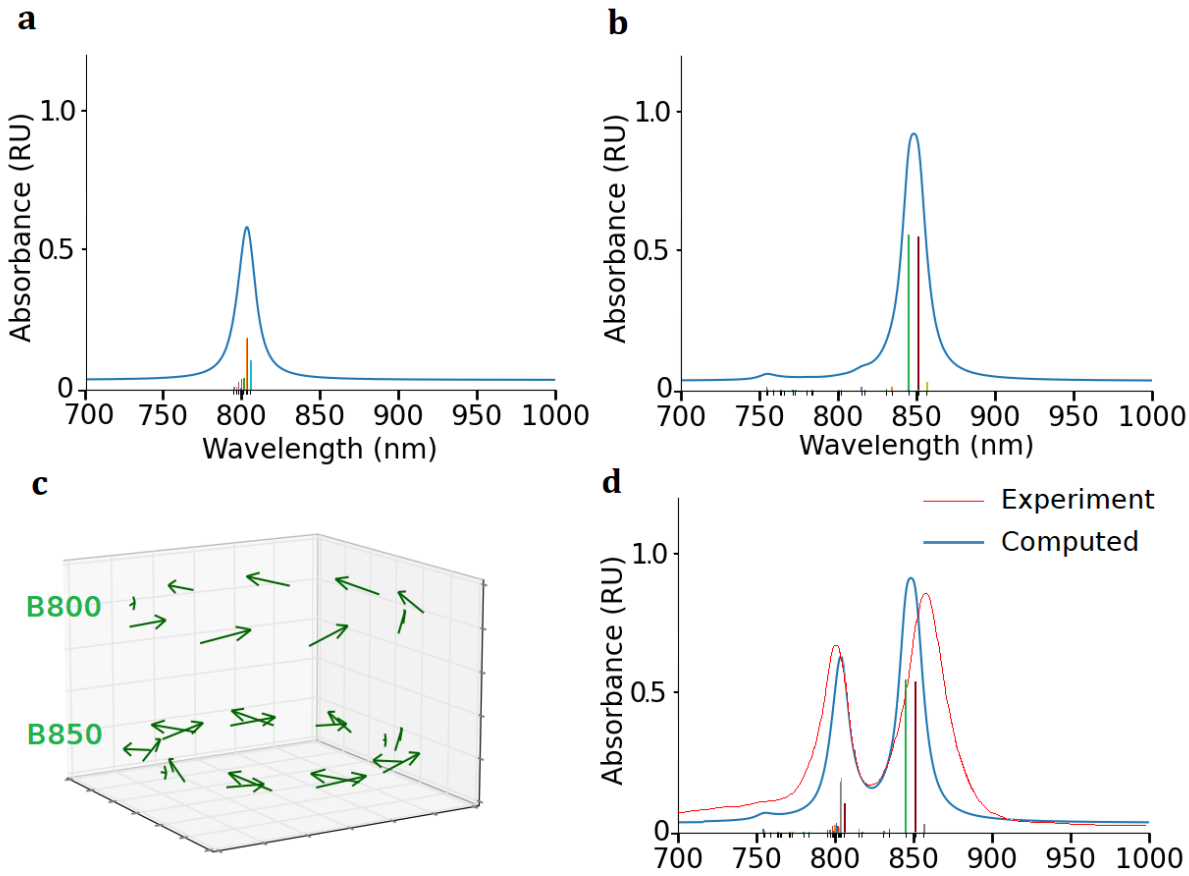

Figure 1: The absorption spectra of the B800 (**a**) and B850 (**b**) rings, the relative positions and orientations of the Bchl a transition dipole moments in the B800 and B850 rings (**c**) and the computed and experimental absorption spectra of the LH2 (**d**). Each absorption signal in the stick-spectra was broadened with Lorentzian distributions centered at the absorption wavelengths of the signals with a half-width at half-maximum (HWHM) of 6 nm. The continuous spectra were then obtained from summing up the contributions of each individually broadened signals. The energies of the states, including those with negligible visibility, are marked with small black lines on the wavelength-axis, so that the B800 states are centered near 800 nm (**a**) and the B850 states more widely distributed in energy (**b**). The magnitudes of the transition dipole moments in **c** are equal, and not related to the spatial dimensions. The experimental spectrum is provided by Fan Wu from the Department of Chemical Physics, Lund.

3.2 Relaxation of the excitons in the LH2

Relaxation of excitons was simulated by numerically solving the relevant equations in Section 2.5 with an initial population corresponding to the excited state of B800 with the highest visibility and with the temperature set to 293 K. In order to evaluate the time-evolution of the populations of B800 and B850 in all of the excitonic states simultaneously, the following

definitions were used

$$p_{B800}(t) = \sum_{\alpha, m \in B800} c_\alpha(m) p_\alpha(t) \tag{3.1}$$

$$p_{B850}(t) = \sum_{\alpha, m \in B850} c_\alpha(m) p_\alpha(t). \tag{3.2}$$

The value of the parameter j_0 in Eq. 2.33 was optimized to $850\hbar$, so that the relaxation from B800 to B850 took about 0.7 ps at room temperature (Fig. 2 inset) - a characteristic which has been obtained in previous experimental studies [45]. The parameter E_0 was set to 100 cm^{-1} as in [28] and the exciton lifetime to the experimental value $\tau_{exc} = 200$ ps, which was provided by Fan Wu from the Department of Chemical Physics, Lund. In order to verify the fast relaxation of 0.7 ps from B800 to B850 and the slower decay to ground state, the simulation was run separately for 7 and 600 picoseconds (Fig. 2).

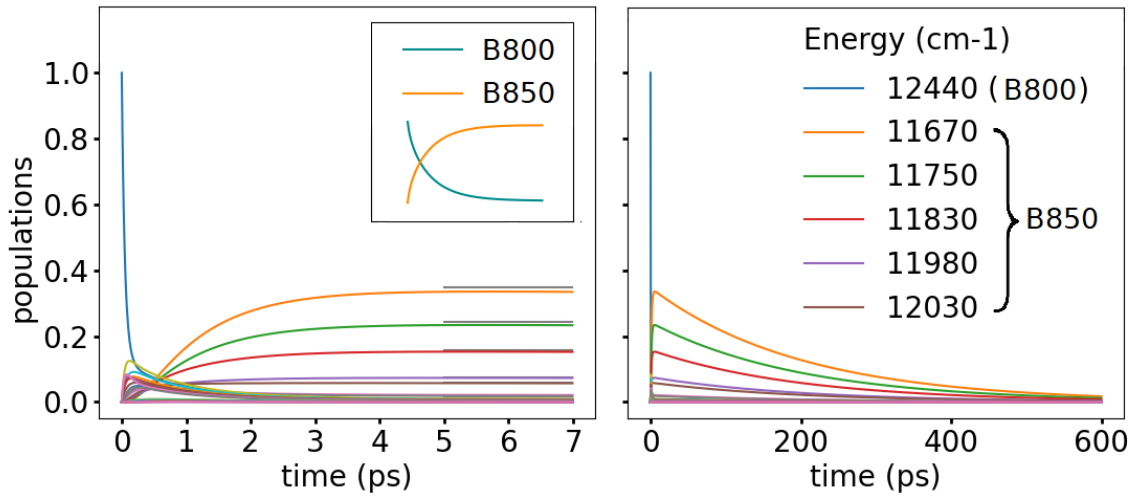

Figure 2: Relaxation of a population of excitons in the B800 state towards the B850 states (left) and the following decay of the populations towards the ground state (right). The grey horizontal lines are the Boltzmann distributed populations given by Eq. 2.36 for each state. Only the 5 lowest energies of the B850 states together with the energy of the initially excited B800 state are shown on the right, rounded to the nearest tens for clarity. The populations of some of the other B800 states increase in the beginning, but remain close to 0 when Boltzmann distributed. The populations of B800 and B850 are determined with Eqs. 3.1-3.2 and shown during the first 7 ps in the inset (left). After 0.7 ps, the population of B850 has reached approximately two thirds, or a factor of $1 - 1/e$ from its maximum value, and after 200 ps the populations of the B850 states have further decayed by a factor of 1/e (right).

4 Simulations involving LH2-cavity polaritons

4.1 Comparison between the molecular and the excitonic pictures

The dispersion curve of the polaritons was constructed as a set of absorption spectra with varying cavity wavelength both in the molecular picture by coupling the cavity to the transition dipole moments of individual chlorophylls as described in Section 2.2 and also by coupling the cavity to excitons as described in Section 2.3. The absorbance, or visibility of each polariton was determined from the relation 2.21. In all simulations, the magnitudes of the transition dipole moments of the chlorophylls, $|\boldsymbol{\mu}_k|$, were set to 1 while the coupling constants E and E' involved in Eqs. 2.18, 2.19 and 2.23 were set to 50 cm^{-1}. To assess the effect of the directionality of the LH2s to the polaritonic spectrum, a single LH2 with the geometry specified in Fig. 1 **c** was used and the direction of the polarization of the cavity mode was varied via employing Eq. 2.18 in specifying the coupling to different molecules in the LH2 (Fig. 3). For comparison, the spectrum of a population of LH2s was computed with the excitonic picture and by changing the basis to the site basis with the help of Eqs. 2.25-2.26 (lower right part of Fig. 3). The average values $\overline{\cos(\theta_k)}$ for different molecular sites varied with $E\overline{\cos(\theta_k)}$ ranging from -100 cm^{-1} to 94 cm^{-1}. LP, MP and UP branches were distinguished as in [18], corresponding to a combination of the dispersion curve of the photonic component and the nondispersive behavour of the B800 and B850 rings.

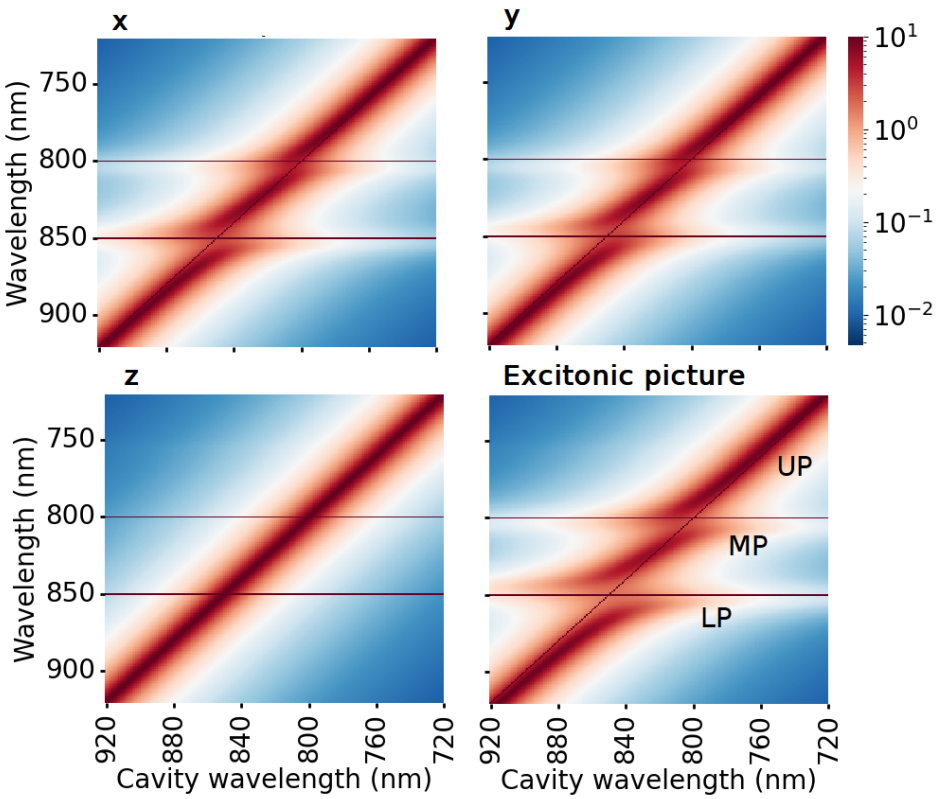

Figure 3: Dispersion curves of a single LH2 in a cavity with the geometry shown in Fig. 1 **c** when the polarization of the cavity mode is parallel to the x, y or z-axis, and the dispersion curve of a population of LH2s computed with the excitonic picture. The heatmaps were obtained by computing the spectra multiple times for different polaritonic Hamiltonians with a fixed cavity wavelength corresponding to the energy $\hbar\omega$ in Eqs. 2.15 and 2.22, determining the absorption intensity from the visibility relation 2.21 and otherwise following the same practice as outlined in Fig. 1 including the use of HWHM of 6 nm. The absorption intensities ranging from about 10^{-2} to 10 units are not comparable between the different plots. The energy of the cavity is shown as a diagonal line, whereas the energies of the B800 and B850 peaks are shown as two horizontal lines. Upper polariton (UP), middle polariton (MP) and lower polariton (LP) branches can be distinguished as in [18].

4.2 The formation of polaritons with a single LH2 in a cavity

To get insight on the formation of the dispersion curve, the energies of the 28 different polaritons, or eigenstates of the polaritonic Hamiltonian (Eq. 2.22), were plotted as a function of cavity wavelength with the excitonic picture and with a single LH2 as previously (Fig. 4 **b**). The HWHM was adjusted to 10 nm and the dispersion curve together with multiple snapshots with a fixed cavity wavelength were plotted with the excitonic picture (Fig. 4 **a** and **c**). The excitonic character in the polaritonic branches was investigated by introducing Hopfield coefficients for

B800 and B850 as

$$|C_{B800}|^2 = \sum_{J,\alpha,n\in B800} |c_J(0)|^2 |c_J(\alpha)|^2 |c_\alpha(n)|^2 \tag{4.1}$$

$$|C_{B850}|^2 = \sum_{J,\alpha,n\in B850} |c_J(0)|^2 |c_J(\alpha)|^2 |c_\alpha(n)|^2 \tag{4.2}$$

$$|C_{cavity}|^2 = \sum_{J} |c_J(0)|^4, \tag{4.3}$$

where $|c_J(0)|^2$ and $|c_J(\alpha)|^2$ are the photonic and excitonic Hopfield coefficients, respectively, and $|c_\alpha(n)|^2$ the expansion coefficients of the excitons (Fig. 4 **d**). The summations include the polaritons $|J\rangle$, polaritonic excitons $|0_c, \alpha\rangle$ and molecules n in either the B800 or the B850 ring.

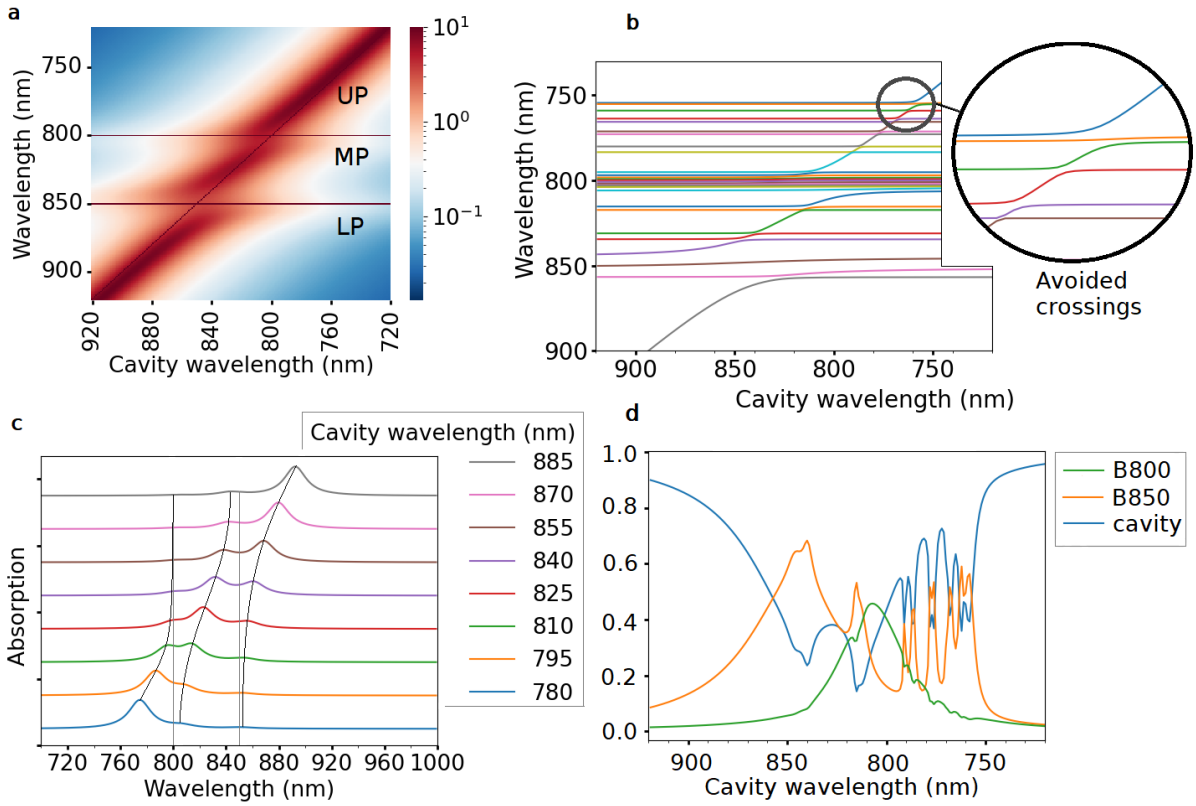

Figure 4: The dispersion curve of the LH2 in a cavity computed with the excitonic picture (**a**), the energies of the 28 polaritons as a function of cavity wavelength (**b**), the absorption spectra with different cavity wavelengths (**c**) and the plots of the Hopfield coefficients of B800, B850 and the cavity (**d**). The polariton energies do not cross, which is seen in the avoided crossings in **b**. The HWHM used in obtaining **a** and **c** is 10 nm. The plots **b** and **d** do not take broadening into account, which can be seen from the abrupt avoided crossings in **b** and in the discontinuous and oscillatory behaviour in **d** at wavelengths where the avoided crossings occur. The energies of some of the dispersionless states (horizontal lines in **b**) correspond to the energies of the B800 states in Fig. 1 **a**, whereas the other dispersionless states correspond to the B850 states in Fig. 1 **b**.

4.3 The formation of polaritons with two LH2s in a cavity

In order to investigate the possibility of exciting multiple LH2s with the excitation of a single polariton branch, the dispersion curve was constructed again with the excitonic picture and with the same coupling constant, but using two LH2s in the Hamiltonian instead of one (Fig.5). The diagonal disorders used in the molecular sites of the two LH2 are shown in Appendix A. In order to evaluate the delocalization of the polaritons among the two LH2s, LH2 a and LH2 b, the following Hopfield constants were introduced:

$$|C_{LH2a}|^2 = \sum_{J,\alpha \in LH2a} |c_J(0)|^2 |c_J(\alpha)|^2 \tag{4.4}$$

$$|C_{LH2b}|^2 = \sum_{J,\alpha \in LH2b} |c_J(0)|^2 |c_J(\alpha)|^2, \tag{4.5}$$

where for example $\alpha \in LH2a$ refers to all of the excitonic Hopfield coefficients of the excitonic LH2 a states. The contribution of the LH2 a and LH2 b to the three polaritonic branches was calculated by plotting the respective Hopfield coefficients as a function of cavity wavelength and including only the polaritons with energies at the wavelengths $\lambda \geq$ 850 nm (LP), $800 < \lambda <$ 850 nm (MP) and $\lambda \leq$ 800 nm (UP) (Fig. 5).

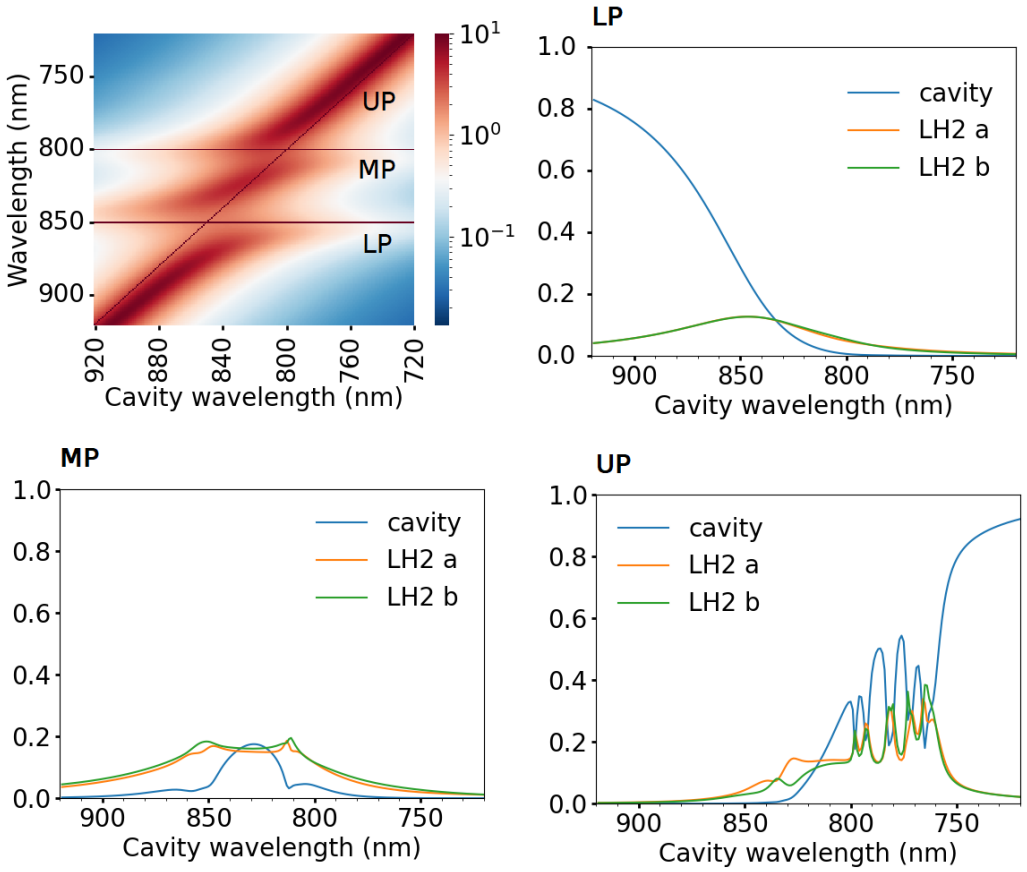

Figure 5: The dispersion curve of two LH2s in a cavity computed with the excitonic picture (upper left) and the Hopfield coefficients of the cavity and the two LH2s when restricted to the polaritonic eigenstates of the LP, MP and UP branches. The diagonal disorders in the two LH2s are given in Appendix A. A HWHM of 10 nm and a coupling constant E' of 50 cm^{-1} are utilized.

4.4 The delocalization and the brightness of individual polaritons

In order to make the following calculations easier, the site basis with the excitonic picture was used with otherwise the same parameters as previously, including the use of the same diagonal disorders for the two LH2s. To compare the polaritonic states with the excitonic states that were computed outside of the cavity in Section 3.1, the dark polaritonic B800 and B850 states that do not contribute to the polaritonic dispersion curve were computed with two LH2s as a function of cavity wavelength from the following definitions

$$|\tilde{C}_{\mathrm{B800}}(J)|^2 = \sum_{m \in \mathrm{B800}} |\mathrm{c_J(m)}|^2 (1 - |c_J(0)|^2), \tag{4.6}$$

$$|\tilde{C}_{\mathrm{B850}}(J)|^2 = \sum_{m\in\mathrm{B850}} |c_{\mathrm{J}}(m)|^2(1-|c_J(0)|^2), \tag{4.7}$$

where $|c_J(0)|^2$ is the photonic Hopfield constant and the sums over the molecules in B800 and B850 include both of the LH2s. The contributions of the B800 and B850 states to the bright polariton states, or the polariton branches, was evaluated with otherwise similar expressions, but with the photonic Hopfield constants, $|c_J(0)|^2$, in place of the factors $1-|c_J(0)|^2$. The dark polariton states corresponded roughly to states close to the energies of the B800 and B850 excitons outside the cavity, whereas the B850 ring contributed to the polariton branches more than the B800 ring (Fig. 6, cf. Fig. 1 and Fig. 4 **b**).

The delocalization of the LH2 a and LH2 b in the polaritons was evaluated with the following expressions of the occupancies in the two LH2s,

$$OCC_{LH2a}(J) = \sum_{m\in LH2a} |c_J(m)|^2 \tag{4.8}$$

$$OCC_{LH2b}(J) = \sum_{m\in LH2b} |c_J(m)|^2. \tag{4.9}$$

The dark polariton states appeared to be highly localized, corresponding to the energies of the LH2 outside the cavity, whereas bright states involved delocalization among the LH2s (Fig. 6). Furthermore, several polariton states contributed to the visibility of any given polariton branch (Fig. 6).

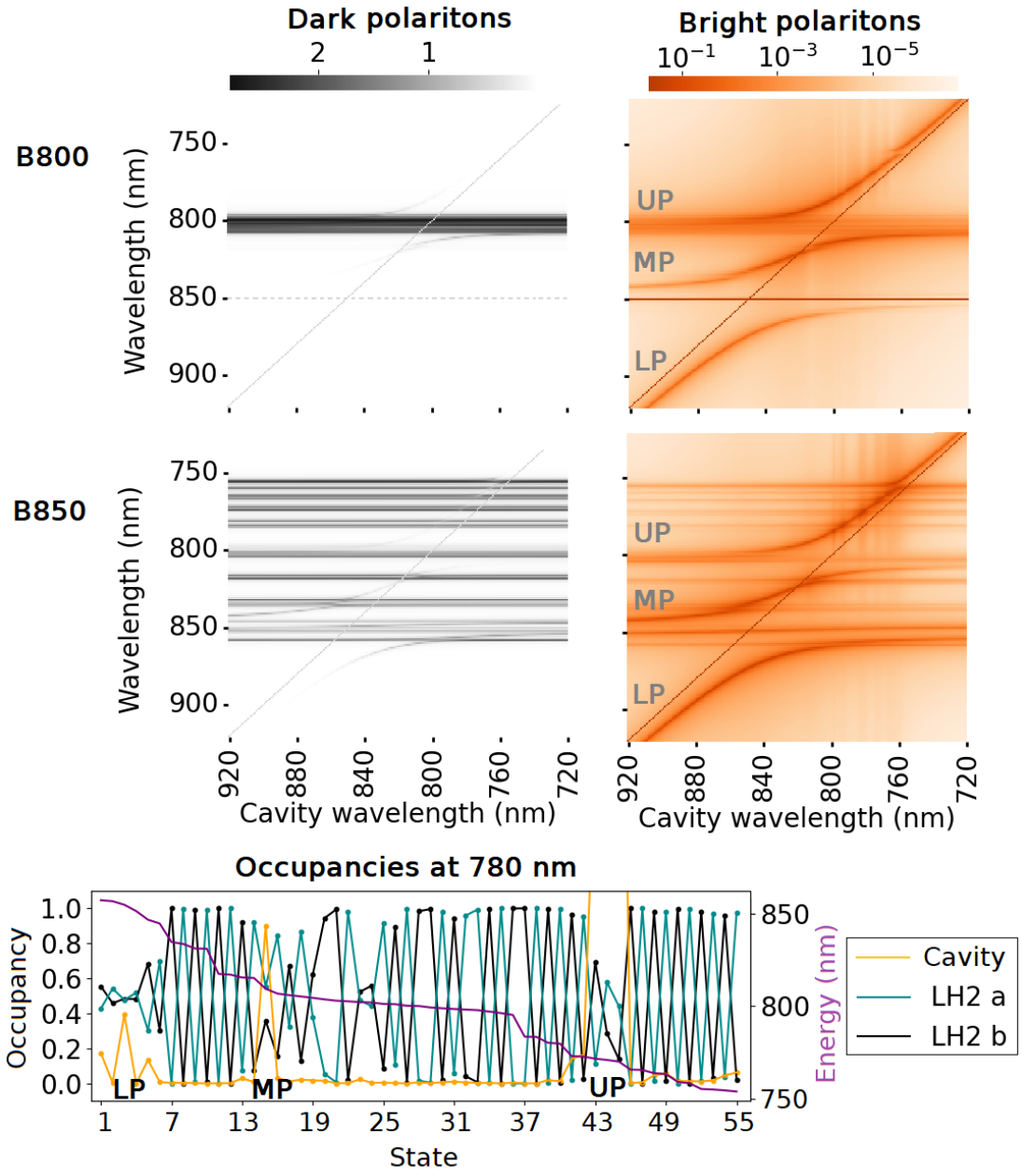

Figure 6: The contribution of the B800 and B850 rings to the dark (black) and bright (orange) polaritons, and the occupancies in the LH2 a and b together with the photonic Hopfield constants (yellow) from the lowest energy state to the highest at cavity wavelength of 780 nm (below). The cavity was scaled by a factor of 10 in the plot below. The dark states were plotted with Eqs. 4.6-4.7 and the bright states in otherwise the same way but using the photonic Hopfield constants in place of the factors $1-|c_J(0)|^2$. To make the states appear more clearly in the heatmaps, they were broadened with a HWHM of 0.5 nm. The magnitudes higher than 1 are due to slight overlap of dark states, whereas the vertical bright lines in the upper right corners of the heatmaps depicting the bright states are due to the erratic behaviour at avoided crossings and the corresponding Lorentzian tails. The small amount of brightness in the dark states is negligible due to the logarithmic scale used in the heatmaps of the bright states.

4.5 Cavity-mediated energy transfer between two LH2s

Relaxation between the two LH2s introduced previously was simulated with and without the cavity (Fig. 7). The Hamiltonian of the two LH2s outside the cavity was constructed otherwise similarly as previously, except that the matrix elements involving the photonic states $|1_c, G\rangle$ were omitted (Section 2.4). When cavity was included, a fixed cavity wavelength of 780 nm was used. The Hamiltonians were constructed in the site basis so that the couplings between the molecules and the cavity were obtained via a change of basis from the excitonic to the site basis with E =50 cm^{-1} as in Section 4.1 (Eqs. 2.25-2.26).

As motivated in Section 2.6, the initially populated state was chosen to be a dark state having occupancy of close to unity in one of the LH2s (LH2 a). The occupancies in the two LH2s were determined with Eqs. 4.8-4.9. The parameters were otherwise kept the same as in the case of a single LH2 described in Section 3.2. To evaluate the transfer from LH2 a to LH2 b explicitly, the following definitions were used for the populations of the two LH2s:

$$p_{LH2a}(t) = \sum_{J,m\in LH2a} c_J(m)p_J(t) \tag{4.10}$$

$$p_{LH2b}(t) = \sum_{J,m\in LH2b} c_J(m)p_J(t), \tag{4.11}$$

where the index J refers to different polariton or exciton states depending on whether the cavity is included. A cavity decay with a lifetime of 14 fs was included in the simulations. A clear transfer between the LH2s in the cavity was observed with strong coupling regardless of the cavity decay, whereas the transfer and the cavity decay was less significant with weaker coupling and absent outside of the cavity (Fig. 7).

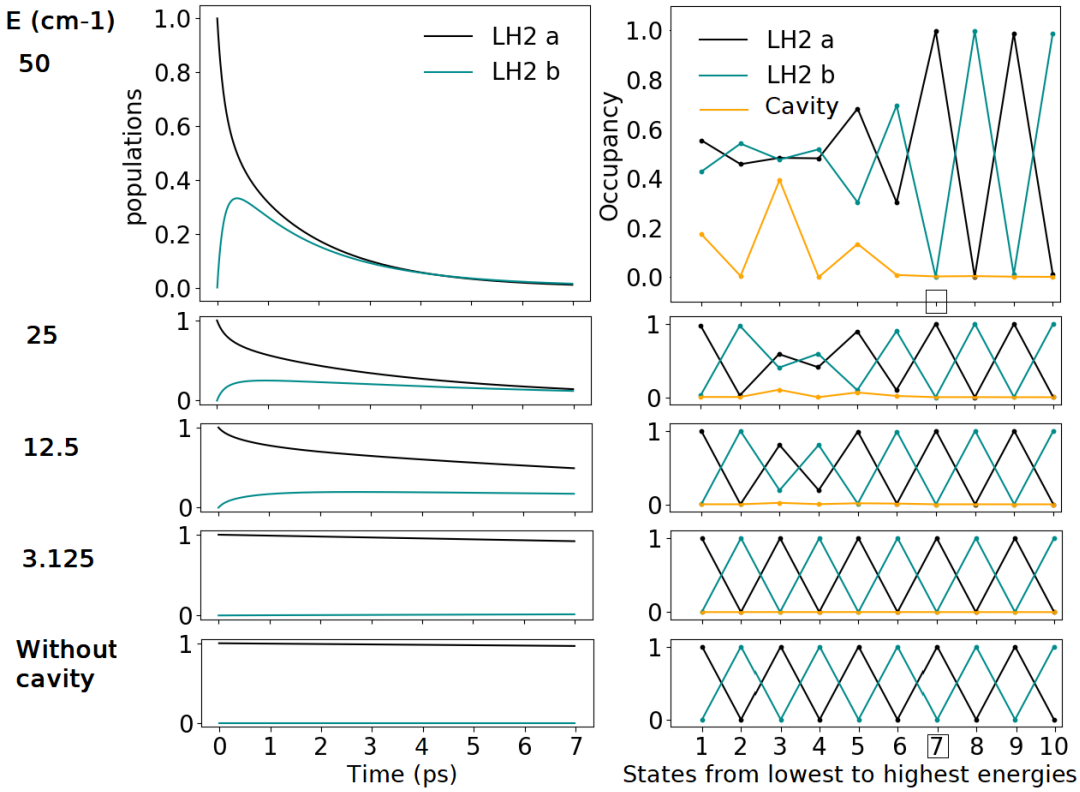

Figure 7: Relaxation from one LH2 (LH2 a) to another (LH2 b) starting from a state with the seventh lowest energy of about 11980 cm^{-1} or $\sim$ 835 nm and with a predominant LH2 a character (right) when the cavity wavelength is 780 nm. The occupancy in the cavity is given by the photonic Hopfield constants of each state (yellow), and scaled by a factor of 10. All of the seven lowest energy states are B850 states (Fig. 6) with a slight photon character in the states 1,3 and 5 in the LP branch (Fig. 6). The coupling constant E (see Section 2.3 and Eq. 2.23) is lower by a factor of 1/2, 1/4 and 1/16 in the three cases below the one with E= 50 cm^{-1}. The cavity lifetime is set to 14 fs, and without the cavity, the slight decay is only due to the exciton lifetime (τ_{exc}). Odd dark states belong to LH2 a and even dark states to LH2 b, which is a coincidence due to the slight differences in the diagonal disorders in the LH2 a and b chlorophyll sites: from the bottom of Fig. 6, it can be seen that such an alternating pattern is not always followed. The differences in E can be thought to arise e.g. from varying the volume of the cavity (Section 2.2).

5 Discussion

Light-matter states appear in cavities as a photon with a suitable energy excites the system from a state $|N_c, G\rangle$ into the polariton state. The physical understanding of the determination of the absorption signal and the excitation mechanism of the polariton branches, however, remains elusive. The rigorous quantum electrodynamical treatment of absorption as outlined in [35] poses difficulties in the case of cavities, because the field modes inside and outside

the cavity have to be treated separately. Thus, an intuitive understanding of the absorption happening directly via a resonant photon entering the cavity appears as a good starting point for understanding the phenomenon, as I have shown in this thesis.

The formation of polaritons requires strong coupling between the cavity and the molecular components, which is not possible if the occupied cavity mode is not close to resonant with the molecular energy levels for coherent energy exchange between the cavity and the molecules to occur [46]. As can be seen from the lack of hybridization when the polarization of the cavity mode is approximately perpendicular to the transition dipole moments of the molecules (cf. Figs. 3 and 1 **c**), a strong enough interaction is also required. Strong coupling causes the excitons with significant transition dipole moments to obtain photonic character, resulting in the appearance of the polariton branches. Because of the mixture of photonic and molecular character, the dispersion curves of polaritons are also mixtures of the dispersion curve of the cavity and the nondispersive behaviour of the molecular states. In the case of LH2s studied in this thesis, the LP and UP branches exhibit the photonic linear dispersion relation far from the excitonic levels, and the three polariton branches appear as the energy of the cavity approaches that of the excitons. With low cavity energies, for example, the MP and UP branches correspond to the energies of the B800 and B850 levels with significant transition dipole moments but then shift closer to the diagonal cavity dispersion curve with increasing photon character. [4, 17]

The molecular picture in which I treated the LH2 as a single molecular unit with well-defined directionality appears to agree rather well with the excitonic picture in which the cavity was coupled to the excitons of a group of LH2s (Fig. 3). An exception is the case with the polarization being perpendicular to the molecular transition dipole moments. I believe that in a population of randomly oriented LH2s, the probability of an LH2 to be oriented perpendicularly to the polarization would be very low: there are many more orientations corresponding more closely to the x- and y-cases in Fig. 1 so that the effective spectrum would nevertheless be the same as with the excitonic picture. With regard to the change of basis, I could have obtained the same spectra as those that I constructed with the molecular picture also by using the excitonic basis with the directed LH2 simply because the change of basis does not affect the spectral observables [47]. On the other hand, the use of the site basis makes most of the computations in this thesis not only computationally significantly quicker for the computer, but also mathematically simpler. For example, the Hopfield constants of the B800 and B850 (Eqs. 4.1-4.2) could have as well been computed with the site basis and with the sums of the form $\sum_n |c_J(n)|^2$ instead of $\sum_{\alpha,n} |c_J(\alpha)|^2 |c_\alpha(n)|^2$.

Since the strong coupling is induced via coupling of the cavity to the transition dipole moments, the stick spectra that specify the magnitudes of the transition dipole moments as in Fig. 1 can be used to evaluate which molecular structures contribute most to the formation of the polariton branches. In the case of the LH2, the B850 excitons have the greatest transition dipole moments. This is not a coincidence, because the 18 chlorophylls in the B850 ring are significantly closer to each other than the chlorophylls in the B800 ring, contributing to delocalized excitons involving multiple B850 chlorophylls [11]. In fact, approximating the B850

chlorophylls as point dipoles might be a slightly crude one and is presumably the reason for the small but noticeable difference in the position of the B850 peak in the experimental spectrum (Fig. 1 **d**). A more accurate spectrum could be also be obtained by averaging spectra over multiple sets of disorders, which in effect occurs in the nature [20]. In any case, it appears that the B850 peak is approximately twice the size of the B800 peak because there are twice as many B850 chlorophylls contributing to the transition dipole moments as B800 chlorophylls.

Because the cavity couples to the transition dipole moments, it is understandable that the B850 states contribute most to the coupling between the excitons and the cavity and the consequent mixing of the polariton states (Figs. 6 and 4 **d**). The Hopfield constants defined for the B800 and B850 rings also clearly verify the requirement for the cavity to be close to resonant with the excitons for the mixing to occur (Fig. 4 **d**). The apparent coupling to the dark states of B850 in the UP branch, however, is likely a consequence of not including cavity broadening, or the uncertainty in the energy of the photon already in the Hamiltonian as in [18]: a photon that is never fully resonant with an exciton with a negligible transition dipole moment would likely also not mix with it. Similarly, the avoided crossings between the dark states and the polariton branches in Fig. 4 **b** and the erratic and discontinuous behaviour of the Hopfield constants at the regions where the anticrossings occur would likely also disappear after the inclusion of the cavity broadening to the Hamiltonian.

In the case of two LH2s instead of one, the slight differences in the excitonic energies due to the different energy disorders smooths out the plots of the Hopfield constants slightly (Fig. 5). The two LH2s contributed about equally to the visibility of the polaritonic branches, confirming the possibility of forming macroscopic states involving hundreds of thousands of LH2s that may be far away from each other within the volume of the cavity (Fig. 5). Furthermore, the individual states exhibited clear delocalization among the two LH2s in the polariton branches, validating that such macroscopic states would likely involve coherent states (Fig. 6).

The delocalized states played a crucial role in making the energy transfer from one LH2 to another possible (Fig. 7). This is exemplified by the lack of transfer in two noninteracting LH2s outside of the cavity, which involve excitonic states that are either localized at one LH2 or the other. With delocalization, the overlap of wavefunctions between the polaritons that are strongly coupled to the cavity makes the transfer from the initial state localized at LH2 a to other states with LH2 b character possible via the phonon bath that is shared by the localized and delocalized states (cf. Eq. 2.32 and Section 2.6). Because the delocalization requires the presence of the cavity, the transfer can be characterized as being cavity mediated. The population in the initial LH2 always remained higher than in the LH2 accepting the energy, because the seven states with the lowest energies and consequently highest populations had on average higher occupancy in the initial LH2 (cf. Figs. 7 and 2). Because the delocalized states appear at the polariton branches with partial photonic character, cavity decay upon the energy transfer cannot completely be avoided. Intriguingly however, some of the states in the polariton branches are delocalized even in the absence of photon character (see also Fig. 6). It appears as if excitons can also mix with unoccupied cavity modes, which presumably is an

indication of a complete energy transfer from the cavity to the molecules. The inclusion of only a single cavity mode to the model, however, is an approximation in and of itself. More general approaches exist [14] and could have an effect on the relaxation dynamics.

6 Conclusion

With the help of numerical computations, I have shown how the central properties of molecular polaritons, namely strong coupling and mixing between the molecules and the photon modes, become evident in the photosynthetic light harvesting complexes placed in a cavity. With such fundamental knowledge on the 'anatomy' of the molecular polaritons of LH2 and the cavity, I have further laid a framework with which energy transfer between LH2s can be studied theoretically. Importantly, I have built the models from ground up, starting from the reconstruction of the well known spectrum of the LH2 outside of the cavity, recreating the known relaxation dynamics from the weakly coupled B800 to the strongly coupled B850 ring within the LH2 and finally using the same parameters with simulations of polaritons when applicable. A logical next step would be to test the relaxation dynamics of LH2-cavity polaritons with time-resolved spectroscopy methods [21].

Strong coupling to a cavity mode is well known to be a fundamental requirement for the formation of polaritons also with biological molecules [4, 46]. I have further pointed out the correlation between the magnitudes of the transition dipole moments of the excitons and the extent to which the cavity mixes with different molecular structures in which the excitons form. Specifically, the B850 ring appears to contribute most to the mixing, exhibiting delocalized excitons with the greatest transition dipole moments. The apparent coupling to the dark B850 states with negligible transition dipole moments, however, is most likely an artifact of the model, which could be avoided if cavity broadening were to be included.

The simulations I have carried out show a possible mechanism with which the energy transfer between photosynthetic molecules could be altered: via phonon-mediated surface hopping between highly delocalized molecular polaritons and localized dark states. The manifold of dark states that remains uncoupled with the cavity is expected to initiate a fast relaxation away from the excited polariton branch before the cavity decays. The unavoidable relaxation to states of lower energy then leads to occupying polaritonic branches of lower energy. The coherence that is initially lost can then be regained via energy transfer from localized states to again highly delocalized, macroscopic states involving thousands of LH2s.

Due to the dependence of strong coupling to the number of chromophores in the cavity, polariton states could potentially be formed by utilizing only a few bacteria, each with multiple LHCs, in the cavity [4]. The bacterium *Rhodopseudomonas acidophila* whose LHC I studied in this thesis has a width of about 1 μm and a length of 2-5 μm [48], making the incorporation into a microcavity viable [4]. The potential to transfer energy between well separated molecules in the

cavity might also make energy transfer between whole photosynthetic bacteria possible. Excess light can be harmful to photosynthetic organisms, which avoid photodamage by dissipating excess excitation energy away from the photosynthetic molecules [49]. The cavity-mediated energy transfer between photosynthetic bacteria and the related delocalized states might alleviate such photodamage via distribution of excitations among multiple bacteria.

References

[1] W. Kühlbrandt, Structure and function of bacterial light-harvesting complexes, *Structure*, **3**, 6, 521–525, 1995. DOI: https://doi.org/10.1016/S0969-2126(01)00184-8.

[2] Y. Song, R. Sechrist, H. H. Nguyen, W. Johnson, D. Abramavicius, K. E. Redding, and J. P. Ogilvie, Excitonic structure and charge separation in the heliobacterial reaction center probed by multispectral multidimensional spectroscopy, *Nat. Commun.*, **12**, 2801, 521–525, 2021. DOI: https://doi.org/10.1038/s41467-021-23060-9.

[3] F. Caruso, S. K. Saikin, E. Solano, S. F. Huelga, A. Aspuru-Guzik, and M. B. Plenio, Probing biological light-harvesting phenomena by optical cavities, *Physical Review B*, **85**, 125424, 2012.

[4] D. M. Coles, Y. Yang, Y. Wang, R. T. Grant, R. A. Taylor, S. K. Saikin, A. Aspuru-Guzik, D. G. Lidzey, J. K.-H. Tang, and J. M. Smith, Strong coupling between chlorosomes of photosynthetic bacteria and a confined optical cavity mode, *Nat. Commun.*, **5**, 1, 1–9, 2014.

[5] F. Fassioli, R. Dinshaw, P. C. Arpin, and G. D. Scholes, Photosynthetic light harvesting: excitons and coherence, *J. R. Soc. Interface*, **11**, 20130901, 127–148, 2013. DOI: http://dx.doi.org/10.1098/rsif.2013.0901.

[6] R. Croce, R. Van Grondelle, H. Van Amerongen, and I. Van Stokkum, *Light harvesting in photosynthesis*, ser. Foundations of Biochemistry and Biophysics. CRC press, 2018, pp. 249–251, 253, 262, 270, 306–307, 451–453, ISBN: 978-1-351-24289-9.

[7] G. D. Scholes, Polaritons and excitons: Hamiltonian design for enhanced coherence, *Proc. R. Soc. A*, **476**, 20200278, 2020. DOI: http://dx.doi.org/10.1098/rspa.2020.0278.

[8] V. May and O. Kühn, *Charge and energy transfer dynamics in molecular systems, 3rd, Revised and Enlarged Edition*, ser. International series of monographs on physics. WILEY-VCH Verlag GmbH Co. KGaA, 2011, pp. 39–40, 67–70, 119–120, 136–139, 174–179, 193–195, 200–201, 298–299, 469, 474, 476–488, 491–492, 540–541, ISBN: 978-3-527-40732-3.

[9] C. J. Bardeen, The structure and dynamics of molecular excitons, *Annu. Rev. Phys. Chem.*, **65**, 1, 127–148, 2014. DOI: 10.1146/annurev-physchem-040513-103654.

[10] E. Ostrumov, C. Jumper, and G. Scholes, Light harvesting strategies inspired by nature, *Photoelectrochemical Water Splitting: Materials, Processes and Architectures,* Royal Society of Chemistry, 389–405, 2013.

[11] G. McDermott, S. M. Prince, A. A. Freer, A. M. Hawthornthwaite-Lawless, M. Z. Papiz, R. J. Cogdell, and N. W. Isaacs, Crystal structure of an integral membrane light-harvesting complex from photosynthetic bacteria, *Nature*, **374**, 517–521, 1995. DOI: https://doi.org/10.1038/374517a0.

[12] M. Hertzog, M. Wang, J. Mony, and K. Börjesson, Strong light–matter interactions: a new direction within chemistry, *Chemical Society Reviews*, **48**, 3, 937–961, 2019.

[13] P. Michetti and G. La Rocca, Polariton states in disordered organic microcavities, *Physical Review B*, **71**, 11, 115320, 2005.

[14] R. H. Tichauer, J. Feist, and G. Groenhof, Multi-scale dynamics simulations of molecular polaritons: the effect of multiple cavity modes on polariton relaxation, *The Journal of Chemical Physics*, **154**, 10, 104112, 2021.

[15] G. D. Scholes, C. A. DelPo, and B. Kudisch, Entropy reorders polariton states, *The Journal of Physical Chemistry Letters*, **11**, 15, 6389–6395, 2020.

[16] D. M. Coles, L. C. Flatten, T. Sydney, E. Hounslow, S. K. Saikin, A. Aspuru-Guzik, V. Vedral, J. K.-H. Tang, R. A. Taylor, J. M. Smith, *et al.*, Polaritons in living systems: modifying energy landscapes in photosynthetic organisms using a photonic structure, *arXiv preprint arXiv:1702.01705*, 2017.

[17] T. W. Ebbesen, Hybrid light–matter states in a molecular and material science perspective, *Accounts of Chemical Research*, **49**, 11, 2403–2412, 2016.

[18] F. Herrera and J. Owrutsky, Molecular polaritons for controlling chemistry with quantum optics, *The Journal of Chemical Physics*, **152**, 10, 100902, 2020.

[19] R. Saez-Blazquez, J. Feist, E. Romero, A. I. Fernández-Domínguez, and F. J. García-Vidal, Cavity-modified exciton dynamics in photosynthetic units, *J. Phys. Chem. Lett.*, **10**, 15, 4252–4258, 2019. DOI: https://doi.org/10.1021/acs.jpclett.9b01495.

[20] B. Valeur, *Molecular fluorescence*. Wiley-VCH Verlag GmbH, 2002, pp. 37–38, 67–68, 72, 356, ISBN: 3-527-29919-X.

[21] R. Berera, R. van Grondelle, and J. T. Kennis, Ultrafast transient absorption spectroscopy: principles and application to photosynthetic systems, *Photosynthesis Research*, **101**, 2, 105–118, 2009.

[22] T.-C. Yen and Y.-C. Cheng, Electronic coherence effects in photosynthetic light harvesting, *ScienceDirect*, **3**, 1, 211–221, 2011. DOI: https://doi.org/10.1016/j.proche.2011.08.028.

[23] B. Bransden and C. Joachain, *Quantum mechanics, 2nd edition*, ser. International series of monographs on physics. Pearson Education Limited, 2000, p. 105, ISBN: 978-0-582-35691-1.

[24] W. Parson, *Modern optical spectroscopy: with exercises and examples from biophysics and biochemistry, 2nd edition*, ser. International series of monographs on physics. Springer, 2015, pp. 129–130, 137, 144, 197, ISBN: 978-3-662-46776-3.

[25] P. Peter Atkins and J. De Paula, *Atkins' physical chemistry, 9th edition*. Oxford University Press, 2010, pp. 250, 352.

[26] S. O. S. Hoyer, *Understanding and manipulating electronic quantum coherence in photosynthetic light-harvesting*. University of California, Berkeley, 2013, pp. 1–2.

[27] M. Fox, *Quantum optics: an introduction*. Oxford University Press, 2006, pp. 154–156, 196, 200–203.

[28] S. Tubasum, M. Torbjörnsson, D. Yadav, R. Camacho, G. Söderlind, I. G. Scheblykin, and T. Pullerits, Protein configuration landscape fluctuations revealed by exciton transition polarizations in single light harvesting complexes, *The Journal of Physical Chemistry B*, **120**, 4, 724–732, 2016.

[29] R. Loudon, *The quantum theory of light, 3rd edition*. Oxford University Press, 2006, pp. 49–50, 139–141, 153, 157–165.

[30] C. J. Foot, *Atomic physics*. Oxford University Press, 2005, vol. 7, pp. 29, 123–128.

[31] C. Gerry, P. Knight, and P. L. Knight, *Introductory quantum optics*. Cambridge university press, 2005, pp. 20, 23–25, 74–76, 82, 90.

[32] J. Larson, Extended Jaynes-Cummings models in cavity QED, Ph.D. dissertation, KTH, 2005, 10.

[33] M. O. Scully and M. S. Zubairy, *Quantum optics*. Cambridge University Press, 1997, pp. 3, 5–7.

[34] S. M. Dutra, *Cavity quantum electrodynamics: the strange theory of light in a box*. John Wiley & Sons, 2005, pp. 106, 175–177.

[35] G. Grynberg, A. Aspect, and C. Fabre, *Introduction to quantum optics: from the semi-classical approach to quantized light*. Cambridge university press, 2010, pp. 8–11, 307, 310, 312, 319, 467–497.

[36] D. G. Lidzey, D. D. Bradley, A. Armitage, S. Walker, and M. S. Skolnick, Photon-mediated hybridization of Frenkel excitons in organic semiconductor microcavities, *Science*, **288**, 5471, 1620–1623, 2000.

[37] M. Sentıs, *Quantum theory of open systems*. ETH, Eidgenössische Technische Hochschule Zürich, Institut für Theoretische Physik, 2002, p. 5.

[38] D. A. Lidar, *Lecture notes on the theory of open quantum systems*. 2020, pp. 88–90.

[39] D. Chandler, *Introduction to modern statistical mechanics*. Oxford University Press, 1987, pp. 62–63.

[40] M. Schröter, S. D. Ivanov, J. Schulze, S. P. Polyutov, Y. Yan, T. Pullerits, and O. Kühn, Exciton–vibrational coupling in the dynamics and spectroscopy of frenkel excitons in molecular aggregates, *Physics Reports*, **567**, 1–78, 2015.

[41] D. V. Schroeder, *An introduction to thermal physics*. Alison Wesley Longman, 2000, p. 223.

[42] W. E. Boyce, R. C. DiPrima, and D. B. Meade, *Elementary differential equations*. John Wiley & Sons, 2017, pp. 373–379.

[43] T. Pullerits, M. Chachisvilis, and V. Sundström, Exciton delocalization length in the B850 antenna of Rhodobacter sphaeroides, *The Journal of Physical Chemistry*, **100**, 25, 10787–10792, 1996.

[44] K. Saito, K. Mitsuhashi, and H. Ishikita, Dependence of the chlorophyll wavelength on the orientation of a charged group: why does the accessory chlorophyll have a low site energy in photosystem II? *Journal of Photochemistry and Photobiology A: Chemistry*, **402**, 112799, 2020.

[45] J. L. Herek, N. Fraser, T. Pullerits, P. Martinsson, T. Polivka, H. Scheer, R. Cogdell, and V. Sundström, B800→ B850 energy transfer mechanism in bacterial LH2 complexes investigated by B800 pigment exchange, *Biophysical Journal*, **78**, 5, 2590–2596, 2000.

[46] D. Dovzhenko, S. Ryabchuk, Y. P. Rakovich, and I. Nabiev, Light–matter interaction in the strong coupling regime: configurations, conditions, and applications, *Nanoscale*, **10**, 8, 3589–3605, 2018.

[47] J. Cao, R. J. Cogdell, D. F. Coker, H.-G. Duan, J. Hauer, U. Kleinekathöfer, T. L. Jansen, T. Mančal, R. D. Miller, J. P. Ogilvie, *et al.*, Quantum biology revisited, *Science Advances*, **6**, 14, eaaz4888, 2020.

[48] N. Pfennig, Rhodopseudomonas acidophila, sp. n., a new species of the budding purple nonsulfur bacteria, *Journal of Bacteriology*, **99**, 2, 597–602, 1969.

[49] R. Wimalasekera, Effect of light intensity on photosynthesis, *Photosynthesis, Productivity and Environmental Stress,* Wiley Online Library, 65–73, 2019.

A Disorders used in the simulations

Disorders a (cm^{-1})	Disorders b (cm^{-1})
228	189
66	118
-11	-31
21	48
94	89
23	11
208	229
-129	-126
-44	-76
-54	-50
-106	-129
23	5
91	82
-44	-21
49	10
43	88
172	199
-24	-47
-46	-39
54	40
-20	2
30	8
252	271
-64	-87
155	157
-18	-7
-29	25

Table 1: The diagonal disorders used in the simulations for each chlorophyll in the LH2 ring. Disorders a are the default disorders used in all other simulations other than those which involved two LH2s. Disorders b are the disorders of the extra LH2. Every third row in the table is a disorder of a chlorophyll in the B800 ring, whereas every 2 preceding terms are the disorders of two chlorophylls in the B850 ring closest to the B800 chlorophyll. Due to symmetry of the B800 and B850 rings, the specific ordering of these groups of 3 disorders within the LH2 is expected to have negligible effect on the spectra. To preserve the correct shape of the LH2 spectrum outside the cavity, the Disorders b were obtained from Disorders a via addition of random numbers to each element from a gaussian distribution with a variance of 30 cm^{-1}.